Are Subject-Specific Models Necessary to Predict Patellar Tendon Fatigue Life? A Finite Element Modelling Study

Colin R. Firminger[1,2,3], Ifaz T. Haider[1,3], Olivia L. Bruce[1,2,3], John W. Wannop[1], Darren J. Stefanyshyn[1,2], W. Brent Edwards[1,2,3]

[1]Human Performance Laboratory, Faculty of Kinesiology, University of Calgary, Canada

[2]Biomedical Engineering Graduate Program, University of Calgary, Canada

[3]McCaig Institute for Bone and Joint Health, University of Calgary, Canada

Corresponding Author: Colin Firminger

Mailing Address: KNB 219, Human Performance Laboratory, University of Calgary, 2500 University Drive NW, Calgary, AB Canada, T2N 1N4

Phone: 403-808-2601

Email: cfirming@ucalgary.ca

Word Count: 5909

Abstract

Patellar tendinopathy is an overuse injury that occurs from repetitive loading of the patellar tendon in a scenario resembling that of mechanical fatigue. As such, fatigue-life estimates provide a quantifiable approach to assess tendinopathy risk and may be tabulated using nominal strain (NS) or finite element (FE) models with varied subject-specificity. We compared patellar tendon fatigue-life estimates from NS and FE models of twenty-nine athletes performing countermovement jumps with subject-specific versus generic geometry and material properties. Subject-specific patellar tendon material properties and geometry were obtained using a data collection protocol of dynamometry, ultrasound, and magnetic resonance imaging. Three FE models were created for each subject, with: subject-specific (hyperelastic) material properties and geometry, subject-specific material properties and generic geometry, and generic material properties and subject-specific geometry. Four NS models were created for each subject, with: subject-specific (linear elastic) material properties and moment arm, generic material properties and subject-specific moment arm, subject-specific material properties and generic moment arm, and generic material properties and moment arm. NS- and FE-modelled fatigue-life estimates with generic material properties were poorly correlated with their subject-specific counterparts ($r^2 \leq 0.073$), while all NS models overestimated fatigue life compared to the subject-specific FE model ($r^2 \leq 0.223$). Furthermore, FE models with generic tendon geometry were unable to accurately represent the heterogeneous strain distributions found in the subject-specific FE models or those with generic material properties. These findings illustrate the importance of incorporating subject-specific material properties and FE-modelled strain distributions into fatigue-life estimations.

Key Words

Patellar tendinopathy; Overuse injury; Finite element modelling; Strain;

Introduction

Patellar tendinopathy is a common overuse injury in athletes that perform rapid knee extension maneuvers such as cutting and jumping. The prevalence of patellar tendinopathy is greater than 30% in elite basketball and volleyball athletes (Lian 2005), and 13% in elite soccer athletes (Bode et al. 2017). While several evidence-based rehabilitation protocols for patellar tendinopathy exist (Rutland et al. 2010; Malliaras et al. 2015), this injury is associated with significant morbidity; approximately one third of athletes with patellar tendinopathy experience symptoms lasting more than six months (Cook et al. 1997). The exact pathophysiology of patellar tendinopathy is unknown; however, microdamage accumulation and degenerative alterations characterised by reduced stiffness are known to play a decided role (Helland et al. 2013; Wiesinger et al. 2020).

The progressive degeneration of tendon stiffness resulting from the accumulation of damage in response to repetitive loading is indicative of mechanical fatigue (Edwards 2018). The fatigue failure of a material is heavily dependent on the magnitude of the applied cyclic load, and biological materials are no exception. Indeed, mechanical fatigue tests of human and animal tendon illustrate strong non-linear correlations between measures of peak cyclic stress or peak initial strain and the number of cycles to failure (i.e., fatigue life) (Wang et al. 1995; Schechtman & Bader 1997; Wren et al. 2003). Using estimations of tendon strain based on biomechanical analysis, we previously used a stress-life approach to predict tendon fatigue failure in running and jumping

activity (Edwards 2018; Firminger et al. 2020). In these studies, the nominal strain of the tendon was estimated from measurements of tendon force, stiffness, and resting length.

One of the main drawbacks of nominal strain (NS) modelling is that it lacks subject-specific geometrical information that may play an important role in fatigue-life estimations. A potential improvement over NS modelling is to incorporate tendon geometry into the strain assessment using the finite element (FE) method. Previous work using FE models of the patellar tendon observed heterogenous strain distributions throughout the tendon, with strain concentrations near the patellar/tibial insertions that were influenced by knee angle (Lavagnino et al. 2008; Wang et al. 2020). At the Achilles tendon, the use of subject-specific versus generic geometry and material properties was shown to alter the location and magnitude of FE-predicted stress (Shim et al. 2014; Hansen et al. 2017; Shim et al. 2019).

Both NS and FE modelling approaches may contain varying degrees of subject-specificity, depending on model assumptions and the choice of data collection methodology. For example, some of this information must be acquired through advanced medical imaging (e.g., magnetic resonance imaging) while other information requires only ultrasound technology and dynamometry. Given the sensitivity of fatigue-life estimations to strain magnitude (Wang et al. 1995; Schechtman & Bader 1997; Wren et al. 2003) it would seem prudent to systematically compare strain and fatigue-life outputs from different modelling approaches and levels of subject-specificity. To this end, we developed FE and NS modelling approaches of varying subject-specificity to systematically examine the sensitivity of subject-specific versus generic geometry and material properties on patellar tendon fatigue-life estimations during maximal

countermovement jumps. The FE models were created with: 1) subject-specific material properties (i.e., hyperelatstic material parameters) and geometry; 2) subject-specific material properties and generic geometry; and 3) generic material properties and subject-specific geometry, while the NS models were created with: 1) subject-specific material properties (i.e., linear stiffness) and moment arm; 2) generic material properties and subject-specific moment arm; 3) subject-specific material properties and generic moment arm; and 4) generic material properties and moment arm. We hypothesized that fatigue-life estimations would be more sensitive to models with generic material properties than generic geometry/moment arms, and that fatigue-life estimations obtained using FE models would be lower, as these accounted for strain concentrations due to tendon geometry and interactions with the patellar and tibial insertion sites.

Methods

Data Collection

A complete description of the experimental methodology used in this study can be found in our previous work (Firminger et al. 2019). Briefly, twenty-nine male basketball athletes (18.9 ± 3.4 yr, 1.90 ± 0.10 m, 77.6 ± 12.7 kg) were recruited from the greater Calgary area to perform maximal countermovement jumps in three commercially-available shoes (adidas AG, Herzogenaurach, Germany) and on three surfaces (Robbins Sport Surfaces, Cincinnati, USA) of varying stiffness while motion capture and force platform data were recorded. Immediately prior to the motion capture session, a dynamometry protocol was performed to estimate subject-specific patellar tendon stiffness. Sagittal and axial magnetic resonance imaging (MRI) scans of each subject's right knee were also obtained using an Optima MR430s 1.5 T scanner (GE Healthcare, Chicago, USA). Participants were seated upright and their right leg was placed in the scanner with their knee

at 10° of flexion. Images were collected using a PD-weighted, fast spin echo sequence (echo time = 30.8 ms, repetition time = 3500 ms, acquisition matrix = 320 × 256, flip angle = 90°, field of view = 140 mm, 22 slices, slice thickness = 3.5 mm, scan time = 4.5 min).

Patellar tendon strain was calculated during takeoff only, as no significant difference in patellar tendon force was found between takeoff and landing in our previous research (Firminger et al. 2019). Subject-specific knee joint kinematics and kinetics were calculated for this analysis by averaging across each of the nine shoe and surface conditions, as no significant differences were observed.

Nominal Strain (NS) Model

Custom Matlab code (version 2019a; Mathworks, USA) was used to estimate patellar tendon force (F_{PT}) from a two-dimensional sagittal-plane model of the knee joint (Scott & Winter 1990):

$$F_{\mathrm{PT}} = \frac{M_{\mathrm{k}} + S_{\mathrm{p}} * PCSA_{\mathrm{MG}} * d_{\mathrm{MG}}}{d_{\mathrm{PT}}} \qquad [1]$$

where M_{k} is the sagittal knee moment (obtained from inverse dynamics), S_{p} is the stress in ankle plantarflexor muscles, $PCSA_{\mathrm{MG}}$ is the physiological cross-sectional area of the medial gastrocnemius, d_{MG} is the moment arm of the medial gastrocnemius muscle about the knee joint center (Visser et al. 1990) and d_{PT} is the patellar tendon moment arm obtained from the sagittal-plane MRI scan.

Nominal strain ($\varepsilon_{\mathrm{nom}}$) of the patellar tendon was calculated as follows:

$$\varepsilon_{\mathrm{nom}} = \frac{F_{\mathrm{PT}}}{k_{\mathrm{PT}} * l_{\mathrm{PT}}} \qquad [2]$$

where k_{PT} is the average tangent stiffness between 90-100% of maximum patellar tendon force measured from dynamometry/ultrasound and l_{PT} is the resting length measured from the sagittal MRI scan. Peak nominal strains were calculated for the following conditions: 1) subject-specific stiffness and moment arm; 2) subject-specific stiffness, generic moment arm; 3) generic stiffness, subject-specific moment arm, and 4) generic stiffness and moment arm. Average values of all subjects' moment arms and stiffness values were used for the generic moment arm and patellar tendon stiffness, respectively.

Finite Element (FE) Model

Patellar tendon, patella, and proximal tibia bone geometries were segmented from MRI scans using Mimics 21.0 (Materialize, Leuven, Belgium). The patellar tendon FE geometry was modelled using quadratic tetrahedral elements with element edge lengths between 0.5-1.0 mm (average of 70587 elements). This edge length range was chosen following a convergence analysis of the median value of maximum principal strain in the tendon, where decreasing the edge length range from 1.0-2.0 mm (9160 elements) to 0.5-1.0 mm (42 646 elements) increased the median maximal principal strain by less than 2%. The patella and tibia bone FE geometries were modelled using linear tetrahedral elements with element edge lengths between 1.0-2.0 mm (averages of 14518 and 91710 elements for the patella and tibia, respectively). Isotropic, hyperelastic material properties were applied to the patellar tendon with a Poisson's ratio of 0.49 (Lavagnino et al. 2008). Neo Hookean, Mooney-Rivlin, and Marlow hyperelastic material models were fit to subject-specific stress-strain data, which was obtained by normalizing patellar tendon forces and displacements from the dynamometry protocol by the average cross sectional area (from the axial MRI scan) and l_{PT}, respectively. A Marlow strain energy potential was ultimately utilized as it displayed the best

fit with the experimental data. The patella and tibia bones were modelled using homogenous isotropic linear elastic material properties, with a Young's modulus of 20 GPa and a Poisson's ratio of 0.3 (Reilly & Burstein 1974). Tie constraints were used to connect the proximal and distal aspects of the patellar tendon with the patella and tibia bones, respectively. Nodes in the distal 2 mm of the tibia were fixed in three dimensions and the patella was rotated to a patella-patellar tendon angle (Schmid et al. 2002) corresponding to the knee angle at the timepoint of maximum patellar tendon force. F_{PT} was distributed across the entire patella in a direction parallel to the long axis of the patellar tendon.

[Figure 1 near here]

A series of FE models were created with varying degrees of subject-specificity as follows: 1) subject-specific geometry and material properties; 2) generic geometry, subject-specific material properties; 3) subject-specific geometry, generic material properties. The bone and tendon geometries of a representative subject were randomly selected to represent the generic tendon geometry, while the generic material properties were calculated by fitting a Marlow hyperelastic model to subject-averaged stress and strain data. All FE models were solved using Abaqus 2019 (Dassault Systèmes, USA)

Fatigue-Life Estimation

A stress-life approach was used to estimate fatigue life from initial strain using relationships from previously published human patellar (Firminger & Edwards 2021) and Achilles tendon (Wren et al. 2003) cyclic loading tests. The fatigue-life data from these tendons were combined because

they illustrated similar mechanical fatigue behavior (Firminger & Edwards 2021). For the NS models, the relationship between the initial peak nominal strain and fatigue life (N_f) was as follows:

$$N_f = 6E^{-5}(\varepsilon_{nom})^{-5.663} \qquad [3]$$

In a similar fashion, we sought to combine the Achilles and patellar tendon cyclic loading data to establish a relationship between initial median strain and fatigue life for the FE models. However, only initial nominal strain data was available for the Achilles tendon. We therefore utilized a correction factor created from the patellar tendon cyclic loading data to estimate the Achilles tendon initial median strain from the initial nominal strain. For the patellar tendon, initial median strain obtained from digital image correlation was on average 1.08 times greater than initial nominal strain, and both measures performed equally well at predicting patellar tendon fatigue life (r^2 = 0.57 for initial median strain and r^2 = 0.59 for initial nominal strain). This correction factor was applied to estimate initial nominal strain from initial median strain of the Achilles tendon, and the following relationship between initial median strain (ε_{med}) and fatigue life was established for the combined patellar and Achilles data:

$$N_f = 9E^{-5}(\varepsilon_{med})^{-5.651} \qquad [4]$$

The initial median strains from the FE models were obtained from the maximum principal strain distribution within the patellar tendon after removing elements near the tied regions of the patella and tibia that would be subject to boundary effects.

Data Analysis

Linear regression analyses were performed in SPSS Statistics (version 26; IBM, USA) on the log-transformed N_f data to investigate the sensitivity of fatigue-life estimations within and between the

NS and FE modelling approaches. First, the sensitivity to the use of generic tendon stiffness and/or moment arm was assessed by comparing log(N_f) estimates from the subject-specific NS model and the generic stiffness, generic moment arm, and both generic stiffness and moment arm NS models, respectively. Similarly, the sensitivity of using generic material properties and/or geometry for the FE modelling approaches was assessed by comparing the log(N_f) estimates from the subject-specific FE model with the generic material property and generic geometry FE models, respectively. Finally, the sensitivity of using the subject-specific FE model versus the various NS modelling approaches was assessed. R-squared values were used to assess the goodness-of-fit and an alpha criterion of $\alpha = 0.05$ was used to assess the significance of the regression model. When a significant relationship was found, 95% confidence intervals (CIs) were calculated for the slope and y-intercept to assess whether these coefficients were significantly different from 1 and 0, respectively. In addition, we visualized the FE model outputs for the three FE modelling approaches to investigate the effect of generic material properties and/or geometry on the distribution of maximum principal strains.

Results

[Table 1 near here]

[Table 2 near here]

Average patellar tendon material properties and geometrical data are presented in Table 1, while the average, maximum, and minimum N_f values for each modelling condition are shown in Table 2. The log(N_f) outputs from the subject-specific NS model were poorly correlated with both the

generic stiffness NS model (r^2 = 0.073, p = 0.156) and the generic stiffness and moment arm NS model (r^2 = 0.028, p = 0.191; Figure 2, Table 3). Alternatively, the subject-specific NS model was significantly correlated with the generic moment arm NS model (r^2 = 0.718, $p < 0.001$). The slope and y-intercept for this relationship were not significantly different from 1 and 0, respectively (Table 3).

[Table 3 near here]

[Figure 2 near here]

Fatigue-life outputs from the subject-specific FE model were poorly correlated with those from FE models with generic material properties (r^2 = 0.004, p = 0.743). However, log(N_f) outputs from the subject-specific FE model were highly correlated with the generic geometry FE model (r^2 = 0.942, $p < 0.001$) with a slope and y-intercept that were not significantly different from 1 and 0, respectively (Figure 3, Table 4).

[Figure 3 near here]

[Table 4 near here]

When comparing the subject-specific FE model with the four NS models, all lines of best fit had slopes that were significantly less than 1 and y-intercepts that were significantly greater than 0 (Figure 4, Table 4). The best correlation was observed with the subject-specific NS model (r^2 = 0.22), followed by the generic moment arm NS model (r^2 = 0.16), while the generic stiffness and

combined generic stiffness/moment arm NS models had the lowest correlations (r^2 = 0.08 and r^2 = 0.10, respectively).

[Figure 4 near here]

Figure 5 shows the strain distributions from the three FE modelling approaches for two representative samples. We observed that FE models with generic material properties had strain distributions that closely resembled those of the subject-specific FE model, however the strain magnitudes were often quite different. On the other hand, FE models using a generic geometry did not capture the unique strain distributions observed in the subject-specific FE model, while the strain magnitudes were generally much more similar.

[Figure 5 near here]

Discussion

In this study, we systematically investigated the effect of subject-specific and generic material properties and/or geometry on fatigue-life estimations made from FE and NS models. When comparing within the respective FE and NS modelling approaches, we discovered that those with generic tendon geometry/moment arms were highly correlated with subject-specific fatigue-life estimates, while those with generic material properties were not. Between modelling approaches, we found that fatigue-life estimates from the subject-specific FE model were moderately correlated with the subject-specific and generic moment arm NS models. However, both regressions had slopes significantly different from 1 and y-intercepts significantly different from 0. These results

indicate that even if a subject-specific NS model is used, fatigue-life estimates may be overestimated when compared to FE modelling approaches.

The NS modeling approach estimated nominal strain by combining inverse dynamics with patellar tendon moment arm and stiffness data collected from dynamometry, EMG, ultrasound, and MRI (Firminger et al. 2019). We found that fatigue-life estimates from NS models with a generic patellar tendon stiffness differed from fatigue-life estimates obtained from a best case NS modelling scenario involving subject-specific values for both stiffness and patellar tendon moment arm. However, NS models with a generic patellar tendon moment arm produced fatigue-life estimates that agreed with those from the subject-specific model. This observation can be explained by the relatively small coefficient of variation (9%) in patellar tendon moment arms from subjects in our study. The average (±SD) patellar tendon moment arms for all subjects was 43.0 ± 4.1 mm, which was within the range reported by previous studies (41.3-53.0 mm) (Krevolin et al. 2004; Tsaopoulos et al. 2006). Alternatively, we observed a large coefficient of variation of 35% for patellar tendon stiffness, likely resulting from age and playing level/training load between subjects (Couppe et al. 2008; O'Brien et al. 2010). Similar coefficient of variation magnitudes have been observed in previous *in vivo* estimations of patellar tendon stiffness (Hansen et al. 2006; Carroll et al. 2008), indicating that using an average stiffness value may grossly over- or underestimate an individual's tendon stiffness, leading to large errors in nominal strain and fatigue-life estimations.

Two previous FE models of the patellar tendon investigated the effect of knee flexion angle on stress and strain distributions (Lavagnino et al. 2008; Wang et al. 2020). These studies illustrated

strain concentrations at the patellar and tibial entheses, with a heterogeneous distribution of strains throughout the tendon midsubstance. Speckle tracking approaches of ultrasound data have also illustrated non-uniform displacements within the patellar tendon during passive knee flexion (Pearson et al. 2014; Lee et al. 2017; Slane et al. 2018). Displacement/strain non-uniformities near the entheses have been postulated to occur due to the interaction of the tendon with its bony endpoints, and this was also observed in our FE models. Furthermore, we observed strain concentrations in the tendon midsubstance, the location of which was highly subject-specific. We attribute the heterogeneity of these distributions to localized changes in tendon geometry, indicating that subject-specific tendon geometry may be important when examining localized tendon mechanics or predicting where failure is likely to occur. The relative strain distributions were not affected by the use of generic material properties, suggesting that if the location (but not the magnitude) of peak strain is desired, FE models with generic material and subject-specific geometry may be used.

While the use of generic material properties in the FE model did not affect the observed strain distribution, it had a large influence on the median strain magnitude and thus the estimate of fatigue life. Using generic tendon geometry had the opposite effect, as it greatly altered the strain distribution but had little influence on the median strain magnitude and fatigue-life estimate. For the purpose of accurately estimating strain magnitude and fatigue life, our results indicate that the use of a generic geometry may be acceptable. From a practical standpoint, this finding illustrates that subject-specific MRI scans may not be necessary to obtain accurate fatigue-life estimates (and median strain values) compared to subject-specific FE models.

When comparing the subject-specific FE model with the NS models, we found that fatigue life was overestimated even when the subject-specific NS model was used. In terms of strain, this result indicates that nominal strains from the NS models were comparatively lower than median strains from the FE models. Again, this can likely be attributed to the influence of tendon geometry and interactions between the patellar tendon and the patellar/tibial entheses observed within the subject-specific FE modelling approach. However, we did observe a significant relationship between the subject-specific FE and NS models, indicating that perhaps this relationship could be used to adjust fatigue-life estimates from subject-specific NS models.

The subject-specific FE modelling approach produced an average fatigue-life estimate of 30 600 cycles, indicating that an athlete could perform approximately 15 300 jumps prior to fatigue failure (i.e., each jump consists of a single takeoff and landing). Based on an average of 62 jumps per hour of playing time (Bahr & Bahr 2014), an average daily playing time of 95 minutes (Rodríguez-Marroyo et al. 2014), and 5 training/playing sessions per week, we estimated that fatigue failure would occur after approximately 31 weeks of activity. At first glance this estimate seems reasonable, however it still does not account for the processes of repair and adaptation that have been observed at the patellar tendon in response to exercise (Langberg et al. 2001; Magnusson et al. 2003). More specifically, tendon stiffness and Young's modulus have been observed to increase in response to strengthening programs, which would act to decrease strain magnitude and increase fatigue-life estimates in our modelling approaches.

Several limitations should be addressed for the context of this study. Most importantly, both the FE and NS modelling approaches have not been validated with experimental data. Fatigue-life

339 estimates rely heavily upon an accurate measure of strain, which we have shown is highly
340 dependent upon the material properties assigned to the tendon. As such, validating *in vivo*
341 estimates of material properties and/or strain may represent a more prudent next step in the
342 development of a framework for estimating patellar tendinopathy risk. However, the average
343 values for stiffness and Young's modulus that we obtained were 3749 ± 1327 $N \cdot mm^{-1}$ and 2.23 ±
344 0.86 GPa, respectively, which are similar to previously-reported values (Kongsgaard et al. 2007;
345 Couppe et al. 2008; Helland et al. 2013). Furthermore, we used equivalent material properties for
346 the FE and NS modelling approaches, so the relative differences between conditions would be
347 similar and unlikely to influence the interpretation of our results. Another limitation of this study
348 was the use of homogeneous material properties across the entire patellar tendon, similar to
349 previous FE modelling studies (Lavagnino et al. 2008; Wang et al. 2020). Several studies have
350 suggested that patellar tendon material properties are location-dependent, differing between the
351 anterior and posterior aspects of the tendon (Basso et al. 2002; Haraldsson et al. 2005). Accounting
352 for these regional differences in material properties may provide more accurate estimates of strain
353 throughout the tendon. In addition, our models treated the estimation of patellar tendon strains as
354 a quasi-static problem and as such did not account for loading rate effects of the tendon during
355 dynamic trials. Although it may be tempting to correct for loading rate in future models, previous
356 research of wallaby tendons illustrated no difference in Young's modulus when loaded to the same
357 stress level between 2.2 Hz and 70 Hz (Wang et al. 1995). In this instance the stress-strain
358 relationship of the tendon would likely be insensitive to changes in loading rate. However, the
359 number of cycles to failure tends to increase with loading rate (Wang et al. 1995), which may be
360 captured in the standard fatigue equation through the use of a correction factor to generate more
361 meaningful fatigue life estimates (Firminger et al. 2020). Finally, we modelled the patellar tendon

with isotropic material properties for the FE models, which has been performed in previous FE models (Lavagnino et al. 2008; Wang et al. 2020) and represents a simplification of the transversely-isotropic material properties that have been observed for tendon (Lynch et al. 2003). However, since we were mainly concerned with strains in the longitudinal direction, we believe the use of isotropic material properties was not a major limitation.

Conclusion

We investigated the effects of using subject-specific versus generic material properties and geometry on two modelling approaches when estimating patellar tendon fatigue life. Within both FE and NS modelling approaches, fatigue-life estimates were highly sensitive to the use of generic material properties, while models with generic geometry were highly similar with their subject-specific counterparts. However, FE models with generic geometry were unable to accurately represent the heterogeneous strain distributions observed in fully subject-specific FE models or those with generic material properties. Furthermore, subject-specific NS models overestimated fatigue life compared to subject-specific FE models, as they are unable to account for unique tendon geometries that gave rise to heterogeneous strain distributions. Compared to NS modelling approaches, FE modelling approaches incorporate the heterogeneity of strains caused by localized geometry and interaction with the patella and tibia, resulting in disparate fatigue-life estimates between approaches.

Conflicts of interest

The authors have no competing or financial interests to disclose.

Funding

Research funding was provided in part by the Natural Sciences and Engineering Research Council of Canada (NSERC; RGPIN 01029-2015, CGSD3 504212-2017), Alberta Innovates (Graduate Studentship # 201810543), and the NBA/GE Healthcare Orthopedics and Sports Medicine Collaboration.

References

Bahr MA, Bahr R. 2014. Jump frequency may contribute to risk of jumper's knee: a study of interindividual and sex differences in a total of 11,943 jumps video recorded during training and matches in young elite volleyball players. Br J Sports Med. 48(17):1322–1326.

Basso O, Amis AA, Race A, Johnson DP. 2002. Patellar tendon fiber strains: their differential responses to quadriceps tension. Clin Orthop Relat Res.(400):246–253.

Bode G, Hammer T, Karvouniaris N, Feucht MJ, Konstantinidis L, Südkamp NP, Hirschmüller A. 2017. Patellar tendinopathy in young elite soccer- clinical and sonographical analysis of a German elite soccer academy. BMC Musculoskelet Disord. 18(1):1–7.

Carroll CC, Dickinson JM, Haus JM, Lee GA, Hollon CJ, Aagaard P, Magnusson SP, Trappe TA. 2008. Influence of aging on the in vivo properties of human patellar tendon. J Appl Physiol [Internet]. 105(6):1907–1915. http://jap.physiology.org/cgi/doi/10.1152/japplphysiol.00059.2008

Cook JL, Khan KM, Harcourt PR, Grant M, Young DA, Bonar SF. 1997. A cross sectional study of 100 athletes with jumper's knee managed conservatively and surgically. The Victorian Institute of Sport Tendon Study Group. Br J Sports Med [Internet]. 31(4):332–336. https://bjsm.bmj.com/lookup/doi/10.1136/bjsm.31.4.332

Couppe C, Kongsgaard M, Aagaard P, Hansen P, Bojsen-Moller J, Kjaer M, Magnusson SP. 2008. Habitual loading results in tendon hypertrophy and increased stiffness of the human patellar tendon. J Appl Physiol. 105(3):805–810.

Edwards WB. 2018. Modeling Overuse Injuries in Sport as a Mechanical Fatigue Phenomenon. Exerc Sport Sci Rev. 46(4):224–231.

Firminger C, Asmussen M, Cigoja S, Fletcher J, Nigg B, Edwards W. 2020. Cumulative Metrics of Tendon Load and Damage Vary Discordantly with Running Speed. Med Sci Sport Exerc.

52(7):1549–1556.

Firminger CR, Bruce OL, Wannop JW, Stefanyshyn DJ, Edwards WB. 2019. Effect of Shoe and Surface Stiffness on Lower Limb Tendon Strain in Jumping. Med Sci Sport Exerc.(10):1.

Firminger CR, Edwards WB. 2021. Effects of cyclic loading on the mechanical properties and failure of human patellar tendon. J Biomech [Internet]. 120(1):110345. https://doi.org/10.1016/j.jbiomech.2021.110345

Hansen P, Bojsen-Moller J, Aagaard P, Kjaer M, Magnusson SP. 2006. Mechanical properties of the human patellar tendon, in vivo. Clin Biomech. 21(1):54–58.

Hansen W, Shim VB, Obst S, Lloyd DG, Newsham-West R, Barrett RS. 2017. Achilles tendon stress is more sensitive to subject-specific geometry than subject-specific material properties: A finite element analysis. J Biomech. 56:26–31.

Haraldsson BT, Aagaard P, Krogsgaard M, Alkjaer M, Magnusson SP. 2005. Region-specific mechanical properties of the human patella tendon. J Appl Physiol. 98:1006–1007.

Helland C, Bojsen-Møller J, Raastad T, Seynnes OR, Moltubakk MM, Jakobsen V, Visnes H, Bahr R. 2013. Mechanical properties of the patellar tendon in elite volleyball players with and without patellar tendinopathy. Br J Sports Med. 47(13):862–868.

Kongsgaard M, Reitelseder S, Pedersen TG, Holm L, Aagaard P, Kjaer M, Magnusson SP. 2007. Region specific patellar tendon hypertrophy in humans following resistance training. Acta Physiol. 191(2):111–121.

Krevolin JL, Pandy MG, Pearce JC. 2004. Moment arm of the patellar tendon in the human knee. J Biomech. 37(5):785–788.

Langberg H, Rosendal L, Kjær M. 2001. Training-induced changes in peritendinous type I collagen turnover determined by microdialysis in humans. J Physiol. 534(1):297–302.

Lavagnino M, Arnoczky SP, Elvin N, Dodds J. 2008. Patellar Tendon Strain is Increased at the Site of the Jumper's Knee Lesion during Knee Flexion and Tendon Loading: Results and Cadaveric Testing of a Computational Model. Am J Sports Med. 36(11):2110–2118.

Lee D, Barrett R, Ryan M, Saxby DJ, Newsham-West R, Obst SJ. 2017. In vivo strain in the deep and superficial regions of the human patellar tendon. Scand J Med Sci Sports. 27(10):1105–1113.

Lian OB. 2005. Prevalence of Jumper's Knee Among Elite Athletes From Different Sports: A Cross-sectional Study. Am J Sports Med. 33(4):561–567.

Lynch HA, Johannessen W, Wu JP, Jawa A, Elliott DM. 2003. Effect of Fiber Orientation and Strain Rate on the Nonlinear Uniaxial Tensile Material Properties of Tendon. J Biomech Eng. 125(5):726–731.

Magnusson SP, Hansen P, Kjaer M. 2003. Tendon properties in relation to muscular activity and physical training. Scand J Med Sci Sport [Internet]. 13(4):211–223. http://www.ncbi.nlm.nih.gov/pubmed/12859603

Malliaras P, Cook J, Purdam C, Rio E. 2015. Patellar tendinopathy: Clinical diagnosis, load management, and advice for challenging case presentations. J Orthop Sports Phys Ther. 45(11):887–898.

O'Brien TD, Reeves ND, Baltzopoulos V, Jones DA, Maganaris CN. 2010. Mechanical properties of the patellar tendon in adults and children. J Biomech [Internet]. 43(6):1190–1195. https://linkinghub.elsevier.com/retrieve/pii/S0021929009006770

Pearson SJ, Ritchings T, Mohamed ASA. 2014. Regional strain variations in the human patellar tendon. Med Sci Sports Exerc. 46(7):1343–1351.

Reilly DT, Burstein AH. 1974. The mechanical properties of cortical bone. J Bone Jt Surg Am

460 [Internet]. 56(5):1001–1022. http://www.ncbi.nlm.nih.gov/pubmed/4603167
461 Rodríguez-Marroyo JA, Medina J, García-López J, García-Tormo J V., Foster C. 2014.
462 Correspondence Between Training Load Executed by Volleyball Players and the One Observed
463 by Coaches. J Strength Cond Res [Internet]. 28(6):1588–1594.
464 https://journals.lww.com/00124278-201406000-00013
465 Rutland M, O'Connell D, Brismée J-M, Sizer P, Apte G, O'Connell J. 2010. Evidence-supported
466 rehabiliitation of patellar tendinopathy. North Am J Sport Phys Ther. 5(3):166–178.
467 Schechtman H, Bader DL. 1997. In vitro fatigue of human tendons. J Biomech. 30(8):829–835.
468 Schmid M, Hodler J, Cathrein P, Duewell S, Jacob H, Romero J. 2002. Is impingement the cause
469 of jumper's knee? Dynamic and static magnetic resonance imaging of patellar tendinitis in an
470 open-configuration system. Am J Sports Med [Internet]. 30(3):388–395.
471 http://onlinelibrary.wiley.com/o/cochrane/clcentral/articles/169/CN-00389169/frame.html
472 Scott S, Winter D. 1990. Internal forces at chronic running injury sites. Med Sci Sports Exerc.
473 22(3):357–369.
474 Shim VB, Fernandez JW, Gamage PB, Regnery C, Smith DW, Gardiner BS, Lloyd DG, Besier
475 TF. 2014. Subject-specific finite element analysis to characterize the influence of geometry and
476 material properties in Achilles tendon rupture. J Biomech. 47(15):3598–3604.
477 Shim VB, Hansen W, Newsham-West R, Nuri L, Obst S, Pizzolato C, Lloyd DG, Barrett RS.
478 2019. Influence of altered geometry and material properties on tissue stress distribution under
479 load in tendinopathic Achilles tendons – A subject-specific finite element analysis. J Biomech
480 [Internet]. 82:142–148. https://doi.org/10.1016/j.jbiomech.2018.10.027
481 Slane LC, Bogaerts S, Thelen DG, Scheys L. 2018. Nonuniform Deformation of the Patellar
482 Tendon During Passive Knee Flexion. J Appl Biomech. 34(1):14–22.

Tsaopoulos DE, Baltzopoulos V, Maganaris CN. 2006. Human patellar tendon moment arm length: Measurement considerations and clinical implications for joint loading assessment. Clin Biomech. 21(7):657–667.

Visser JJ, Hoogkamer JE, Bobbert MF, Huijing PA. 1990. Length and moment arm of human leg muscles as a function of knee and hip-joint angles. Eur J Appl Physiol Occup Physiol. 61(5):453–460.

Wang K, Hosseinnejad SH, Jabran A, Baltzopoulos V, Ren L, Qian Z. 2020. A biomechanical analysis of 3D stress and strain patterns in patellar tendon during knee flexion. Int j numer method biomed eng. 36(9):1–11.

Wang XT, Ker RF, Alexander RM. 1995. Fatigue rupture of wallaby tail tendons. J Exp Biol [Internet]. 198(3):847–852. https://journals.biologists.com/jeb/article/198/3/847/6899/Fatigue-rupture-of-wallaby-tail-tendons

Wiesinger HP, Seynnes OR, Kösters A, Müller E, Rieder F. 2020. Mechanical and Material Tendon Properties in Patients With Proximal Patellar Tendinopathy. Front Physiol. 11(June):1–11.

Wren TAL, Lindsey DP, Beaupre GS, Carter DR. 2003. Effects of creep and cyclic loading on the mechanical properties and failure of human Achilles tendons. Ann Biomed Eng. 31(6):710–717.

Tables

Table 1: Average (SD) patellar tendon properties used in the NS models

Stiffness, k_{PT} (N/mm)	Initial length, l_{PT} (mm)	Cross-sectional area (mm^2)	Moment arm (mm)
3749 (1327)	52.9 (9.7)	105.6 (15.4)	43.0 (4.1)

Stiffness was calculated as the average tangent stiffness between 90-100% of maximum patellar tendon force. Initial length, cross-sectional are, and moment arm were all calculated from axial/sagittal MR images.

Table 2: Average (SD), maximum, and minimum fatigue life estimates from each modelling condition

	FE models			**NS models**			
Model type	Subject-specific	Generic material properties	Generic geometry	Subject-specific	Generic material properties	Generic moment arm	Generic material properties & moment arm
Average N_f (±SD)	30608 ± 102530	5442 ± 226667	76271 ± 3933	181649 ± 292392	146459 ± 280895	92541 ± 93832	123557 ± 235777
Min N_f	238	651	495	2843	2214	322	1987
Max N_f	558183	17166	1183077	1407925	1418924	721349	1282730

Table 3: Average values (95% confidence interval) for linear regressions (y = mx+b) between NS modelling approaches to estimate fatigue life.

Subject-specific NS model versus:	**NS models** Generic stiffness	Generic moment arm	Generic stiffness & moment arm
r^2	0.073	0.718*	0.028
slope	0.27 (-0.11, 0.65)	1.06 (0.80, 1.32)	0.23 (-0.12, 0.58)
y-intercept	3.37 (1.51, 5.24)	-0.68 (-1.96, 0.59)	3.59 (1.87, 5.31)

* Indicates a statistically significant regression model ($p < 0.05$)

519 Table 4: Average values (95% confidence interval) for linear regressions (y = mx+b) between FE and NS modelling approaches to

520 estimate fatigue life.

Subject-specific FE model versus:	**FE models**		**NS models**			
	Generic material properties	Generic geometry	Subject-specific	Generic stiffness	Generic moment arm	Generic stiffness & moment arm
r^2	0.004	0.942*	0.223*	0.081	0.162*	0.101
slope	0.03 (-0.15, 0.20)	1.06 (0.95, 1.17)	0.40 (0.11, 0.70)	0.24 (-0.08, 0.57)	0.43 (0.04, 0.81)	0.25 (-0.04, 0.55)
y-intercept	3.51 (2.84, 4.18)	0.10 (-0.30, 0.50)	3.34 (2.22, 4.47)	3.78 (2.55, 5.02)	2.84 (1.38, 4.30)	3.77 (2.65, 4.89)

521 * Indicates a statistically significant regression model ($p < 0.05$)

522

Figure Captions

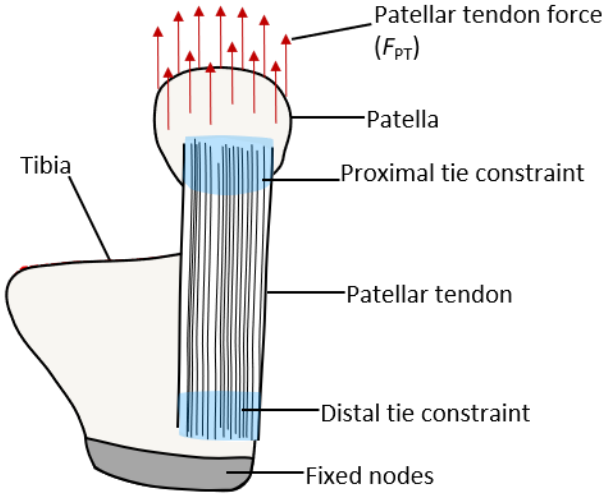

Figure 1: Schematic of the finite element modelling setup. Prior to loading, the patellar tendon was rotated to a patellar tendon-patella angle corresponding to the timepoint of maximum patellar tendon force. Tie constraints were used to connect the patella and tibia to the patellar tendon, and the distal 2 mm of the tibia was constrained in three dimensions. Lastly, patellar tendon force was distributed across the entire patella in a direction parallel to the long axis of the patellar tendon.

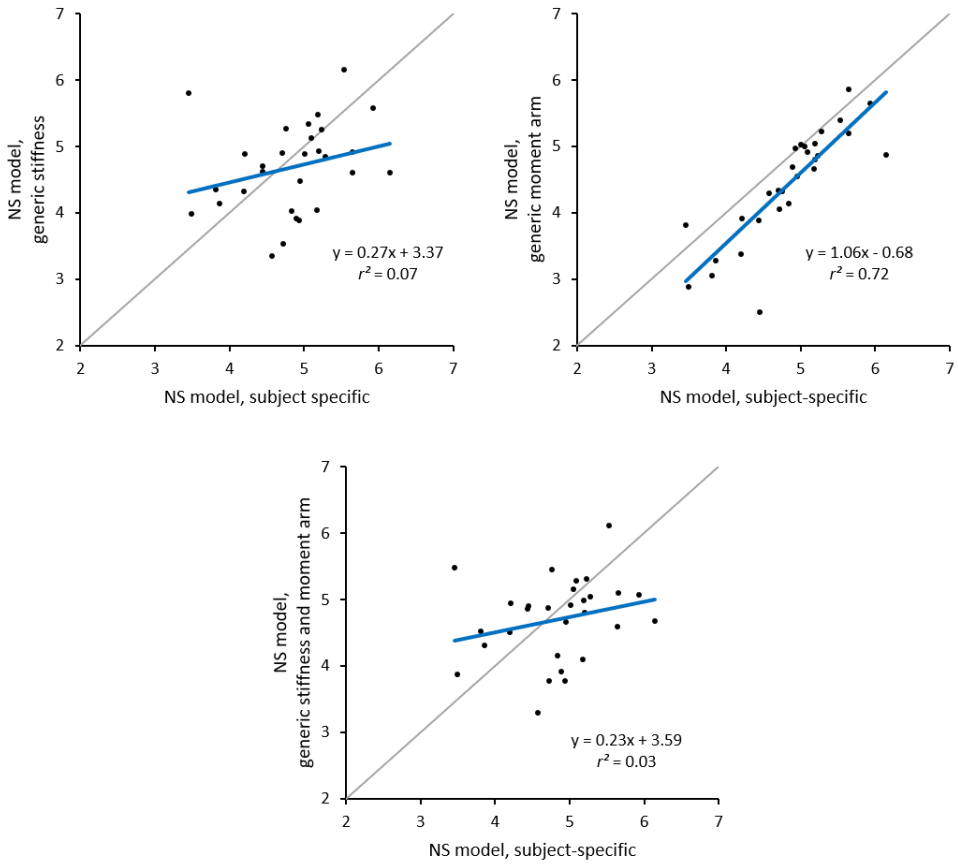

531

532 Figure 2: Logarithmic fatigue-life estimates from the subject-specific NS model compared to NS
533 models with: generic stiffness (top left); generic moment arm (top right); and generic stiffness and
534 moment arm (bottom). The grey line illustrates an x = y relationship for reference.

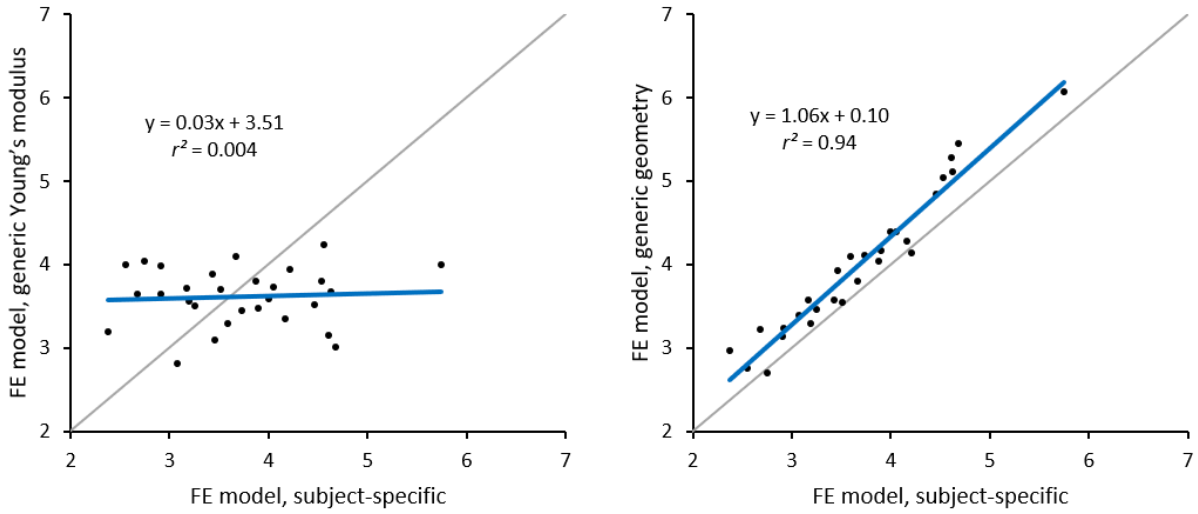

535

536 Figure 3: Logarithmic fatigue-life estimates from the subject-specific FE model compared to FE
537 models with: generic material properties (left); generic geometry (right). The grey line illustrates
538 an x = y relationship for reference.

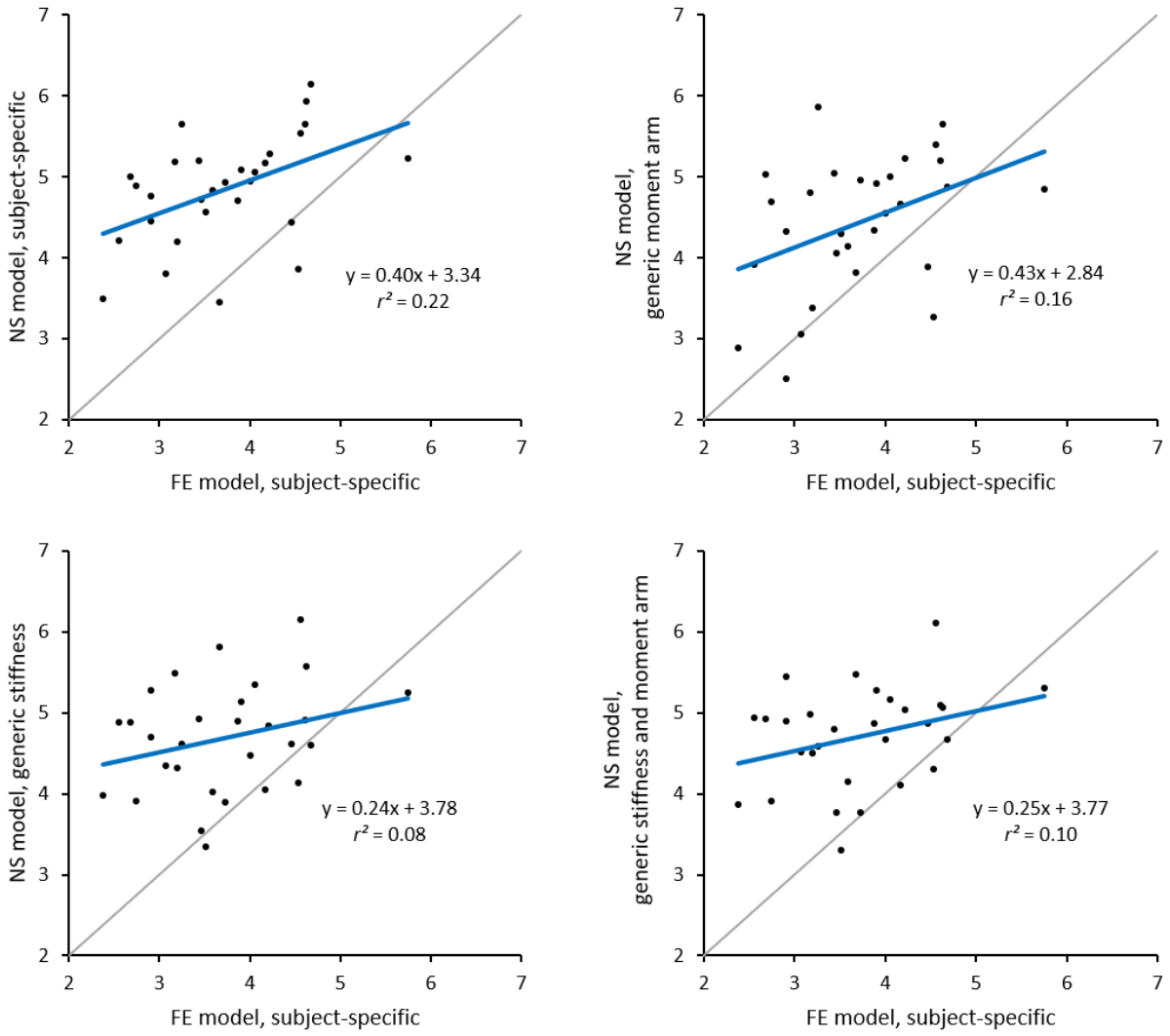

539

540 Figure 4: Logarithmic fatigue-life estimates from the subject-specific FE model compared to NS
541 models with: full subject-specificity (top left); generic stiffness (top right); generic moment arm
542 (bottom left); and generic stiffness and moment arm (bottom right). The grey line illustrates an x
543 = y relationship for reference.

544

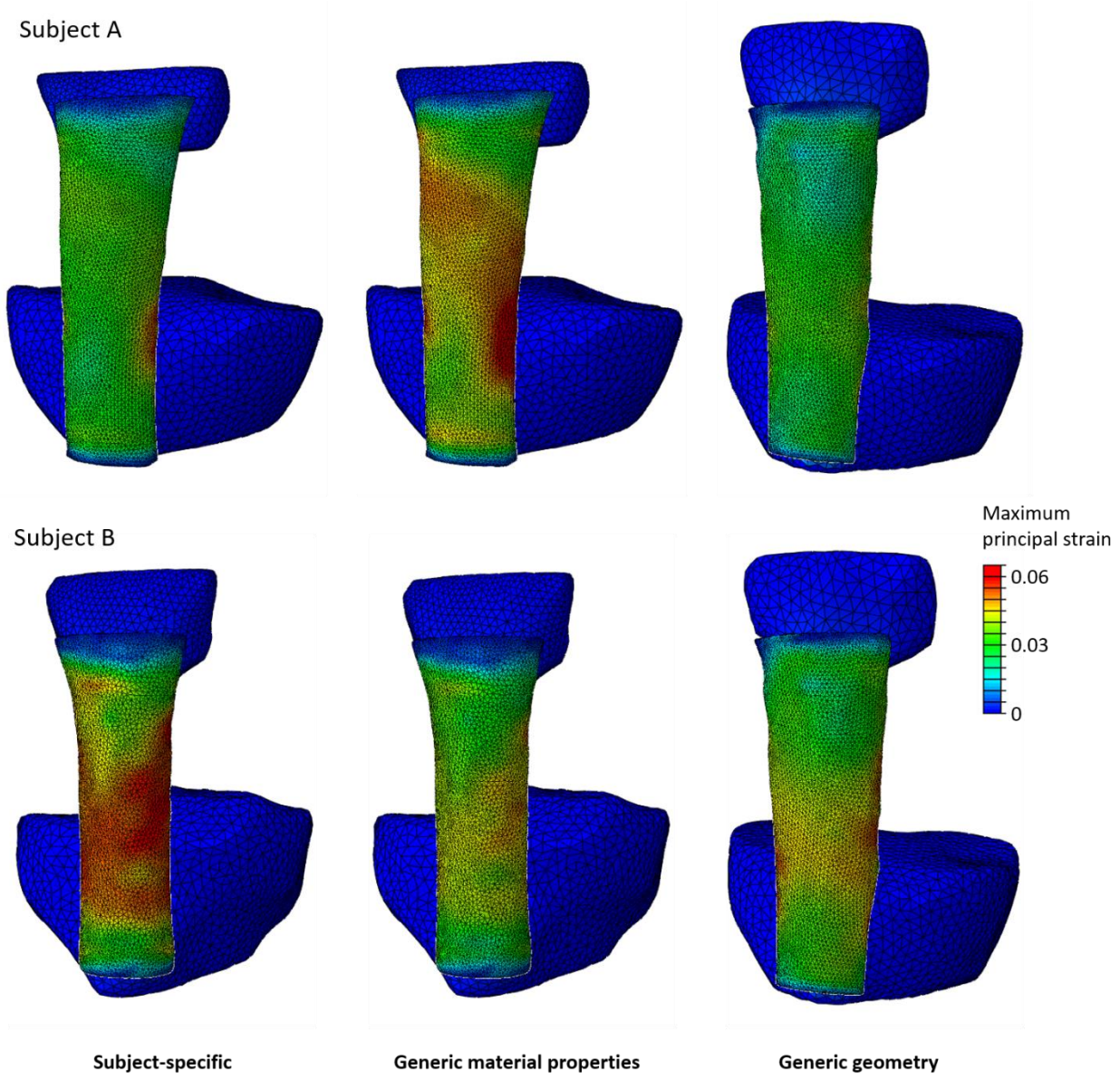

545

546 Figure 5: Maximum principal patellar tendon strain distributions for representative FE models of
547 two subjects, separated by row. Compared to FE models with subject-specific material properties
548 and geometry (right), FE models with generic material properties (middle) had similar strain
549 distributions while FE models with generic geometry (left) had similar median strain magnitude.

550